

A Point-Based Neural Network for Real-Scenario Deformation Prediction in Additive Manufacturing

Meihua Zhao¹, Gang Xiong², *Senior Member, IEEE*, Weixing Wang³,
Qihang Fang⁴, Zhen Shen⁵, *Member, IEEE*, Li Wan⁶, Fenghua Zhu⁷

Abstract—In additive manufacturing (AM), accurate prediction for the deformation of printed objects contributes to compensation in advance, which is crucial to improving the accuracy of products. Many factors affect the deformation, such as the shape of the object, the properties of the material, and parameters in the printing process. Existing methods suffer from difficulties in modeling and generalizing between different shapes. In this paper, we formulate the error prediction in AM as a point-wise deviation prediction task and propose a point-based deep neural network to learn the complex deformation patterns by local and global contextual feature extraction. Furthermore, a data processing flow is proposed for automatically handling the real-scenario data. As an application case, we collect a dataset of dental crowns fabricated by the digital light processing 3D printing and validate the proposed method on the dataset. The results show that our network has a promising ability to predict nonlinear deformation. The proposed method can also be applied to other AM techniques.

I. INTRODUCTION

Additive manufacturing (AM), also known as 3D printing and rapid prototyping, is a technology for manufacturing parts from digital models by stacking materials layer by layer. One of the advantages of AM is its ability to manufacture products with complex structures, such as ceramic cores for hollow aeroengine turbine blades, which are difficult or

even impossible to fabricate with conventional techniques. In addition, without the requirements for molds, fixtures, and intermediate steps, AM makes it possible to manufacture small quantities of products with great diversity and geometric complexity, bringing about a paradigm shift from mass production to individual customization.

Improving the accuracy of printed parts is a fundamental research problem in AM. The more accurate the manufactured parts, the higher their usability. The errors in conventional subtractive manufacturing such as lathe are mainly thermal errors and geometric errors caused by tool path limitations. Because of the existence of mature servo systems, the errors in this technology can be easily controlled at the micron level. However, the AM process is complex. Taking digital light processing (DLP) 3D printing as an example, the manufacturing process usually involves heating, cooling, bonding, and resin curing. The accuracy of its products is affected by a variety of factors, such as optical power, layer thickness, material properties, and part shape. Even if the positioning deflections of a 3D printer are in tens or hundreds of microns, the errors of printed parts are always much larger.

Physics-based modeling, prescriptive modeling, and machine learning methods are three popular approaches for deformation prediction and compensation in AM. Although physics-based modeling has always been a research concern, accurate simulations are difficult and computationally expensive due to the complexity of the AM process. Prescriptive modeling approaches learn error functions from a limited number of shapes and obtain optimal compensation plans for new and untested ones. However, it is difficult to take the effect of inter-layer stresses into account. At present, machine learning-based AM error compensation methods are drawing increasing attention. Some of these methods [1], [2] perform point-level predictions, ignore the understanding of 3D shapes, and are therefore difficult to generalize to other shapes. Also, foundation work is required for error prediction. In our previous work, we proposed an end-to-end error compensation framework and presented a voxel-based neural network for error prediction and compensation [3], [4]. Since the geometric errors of AM parts are much smaller than their sizes, the voxel grid needs to be set to a high resolution for high accuracy error prediction, and the memory burden caused by the voxel representations is heavy. In addition, limited by the accessibility of real datasets, the method uses simple simulation data, which makes it difficult to capture the complex deformations of real-scenario AM

*This work was supported in part by the National Key Research and Development Program (No. 2018YFB1700200), the National Natural Science Foundation of China under Grants U1909218; Scientific Instrument Developing Project of the Chinese Academy of Sciences (Grant No. YZQT014); CAS Key Technology Talent Program (Zhen Shen); Guangdong Basic and Applied Basic Research Foundation under Grant 2021B1515140034; Foshan Science and Technology Innovation Team Project (2018IT100142); Youth Foundation of the State Key Laboratory for Management and Control of Complex Systems (Y6S9011F1G); CAS STS Dongguan Joint Project 20201600200072. (Corresponding author: Zhen Shen.)

¹M. Zhao and ⁴Q. Fang are with the State Key Laboratory for Management and Control of Complex Systems, Institute of Automation, Chinese Academy of Sciences, Beijing 100190, China, and also with the School of Artificial Intelligence, University of Chinese Academy of Sciences, Beijing 101408, China (e-mail: zhaomeihua2018@ia.ac.cn, fangqihang2020@ia.ac.cn).

²G. Xiong is with Beijing Engineering Research Center of Intelligent Systems and Technology, Institute of Automation, Chinese Academy of Sciences, Beijing 100190, China, and also with Guangdong Engineering Research Center of 3D Printing and Intelligent Manufacturing, Cloud Computing Center, Chinese Academy of Sciences, Dongguan 523808, China (e-mail: gang.xiong@ia.ac.cn).

³W. Wang, ⁵Z. Shen, and ⁷F. Zhu are with the State Key Laboratory for Management and Control of Complex Systems, Institute of Automation, Chinese Academy of Sciences, Beijing 100190, China, and also with the Intelligent Manufacturing Center, Qingdao Academy of Intelligent Industries, Qingdao 266109, China (e-mail: weixing.wang@ia.ac.cn, zhen.shen@ia.ac.cn, fenghua.zhu@ia.ac.cn).

⁶L. Wan is with Ten Dimensions (Guangdong) Technology Co., Ltd., Foshan 528225, China (e-mail: li.wan@10dim.com).

parts.

In this paper, we have made further improvements to our previous work. The error prediction task is formulated as a point-wise deviation prediction problem, in which each point in the printed model is considered to be obtained by deforming its corresponding point in the designed model. Therefore, our task is to find the deviation between the two points. Further, we propose a point-based network that extracts multi-level and multi-scale deep features for each point of the input to predict point-wise deviation. The proposed network enables 3D shape understanding by context-aware geometry learning and thus has a good generalization ability to various shapes. Moreover, the memory burden caused by the voxel-based approach can be greatly released. Also, we collect a dental crown dataset manufactured by a DLP 3D printer and provide a data processing flow to obtain the aligned designed model and the printed model. In summary, this work intends to make the following contributions.

- 1) It formulates the error prediction in AM as a point-wise deviation prediction task and proposes a point-based context-aware deep neural network to predict point-wise deviation. The proposed network can generalize to various 3D shapes with a smaller memory burden.

- 2) It collects a real-scenario dataset and proposes a data processing flow. In this way, the complex deformation patterns can be recorded fully.

- 3) It conducts experiments on the collected dataset, and the experimental results demonstrate that the proposed approach can achieve promising results.

The rest of the paper is organized as follows. In Section II, the related work is reviewed. In Section III, we formulate the error prediction task as a point-by-point deviation prediction problem. In Section IV, we introduce the process of real-scenario dataset acquisition. In Section V, we detail the error prediction method and the adopted neural network. In Section VI, we provide the experimental results and analysis. The conclusion is given in Section VII.

II. RELATED WORK

In this paper, we categorize deformation prediction and compensation approaches for AM into physics-based modeling, prescriptive modeling, and machine learning methods.

The complexity of DLP lies in that it is a multi-physics and multi-scale process, including resin-Ultraviolet light interactions at the microscale, the liquid monomers curing at the mesoscale, and thermal-mechanical coupling at the macroscale. Great efforts have been made to develop various physical models to obtain the geometric deformation of the products. Westbeek et al. [5] proposed a multi-physical modeling framework to predict the deformed geometry of vat photo-polymerized components. However, the effects of the resin components contents (i.e., photoinitiators and photoabsorbers) on shape distortion were not considered. Zhang et al. [6] established a material constitutive model to study the development of shape distortion due to volume shrinkage during printing. Given the lack of in-depth understanding of the AM process, it is difficult for the

aforementioned approaches to take all factors of the whole process into account. As a result, predicting the geometry errors accurately in a short time by these physics-driven methods is challenging.

A series of studies established prescriptive models to predict the deformations of AM parts. In 2015, Huang et al. [7] developed a mathematical model of the error in the polar coordinate system and derived an optimal shrinkage compensation function. The error model was only applicable to cylindrical shapes. In their following work, the error prediction model was extended to polygonal shapes and arbitrarily complex shapes [8], [9]. However, the model only models 2D shape deviations and does not consider the effect of inter-layer stresses. Given this, Jin et al. [10] made improvements by modeling out-of-plane deviation for improving the understanding of inter-layer interactions. Since specifying function bases in the normalized model is usually heuristic, this method tends to result in a large uncertainty when predicting the shape deformation of untested products. Considering this problem, Sabbaghi et al. [11] proposed an adaptive Bayesian approach by combining a small set of models manufactured previously with different shapes and their in-plane deviation data to assist in prescriptive modeling of in-plane deviations for a large class of new shapes. Although the prescriptive modeling approaches have been studied a lot, it still suffers from the difficulties of modeling and generalizing to other shapes.

Machine learning-based methods for error prediction and compensation in AM come to the spotlight in recent years. Chowdhury et al. [1] proposed an artificial neural network (ANN) to compensate for the geometric thermal deformation of a part. Similarly, Hong et al. [2] introduced an ANN-based method to compensate for geometric errors in sub-millimeter overhang trusses fabricated by selective laser melting (SLM). During training, the polar angle and radii from the geometric center of the as-printed point cloud were treated as input, and the polar radii of the as-designed point cloud with the same polar angle were regarded as the ground truth. However, the above two methods rely on the finite element method (FEM) or preprinted models to obtain predicted or realistic deformations of 3D parts. In addition, only point-level features are extracted for the prediction, causing the difficulties of extending to other shapes. Huang et al. [12] proposed a shape deviation generator under a convolution formulation, in which the 3D deformation is described as the result of fusing the 2D in-plane deformation with a transfer function that captures the interactions between the layers. The framework has been validated with spherical shapes built in a stereolithography (SLA) process. However, fundamental work is still needed to predict complex deformation patterns of free shapes. Wang et al. [13] extended the above convolutional learning framework to a broader class of 3D geometries by constructively merging spherical and polyhedral shapes into a unified model. Francis and Bian [14] proposed a deep learning-based model to predict the point-wise distortion in 3D printing, which combined a convolutional neural network (CNN) and an ANN for analyzing

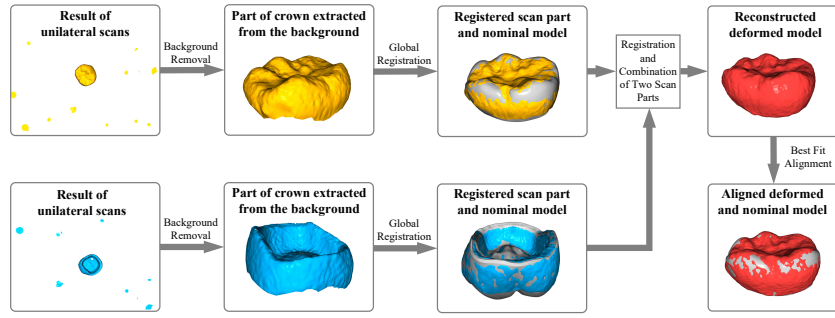


Fig. 1. Data flow diagram for dataset acquisition

thermal images and relevant process/design parameters.

In summary, there is still a lack of an efficient error prediction and compensation approach that can efficiently capture the complex deformation patterns of AM parts and applicable to various shapes. In this paper, in contrast to the point-level prediction, we apply a neural network with local and global contextual feature awareness for error prediction in AM and propose a data processing flow for real dataset collection.

III. PROBLEM STATEMENT

Following the notations in [3], we denote a designed dental crown model as the “nominal model” V and the model output by a particular 3D printer as the “deformed model” V' . To transform them into a form that can be directly processed by the neural network, Poisson sampling is performed on the surfaces of V and V' to obtain “nominal point cloud” P and “deformed point cloud” P' , respectively. It is considered that each item p' in the point cloud P' is obtained by deforming the corresponding point p in the point cloud P , i.e., $p' = p + \Delta p$, where Δp is the vector of point-by-point deviation.

Therefore, the point cloud P is taken as input, and the deviations of all points are predicted by the neural network. Then we add the predicted deviations to the coordinates of points in P for obtaining the predicted point cloud P'' . Our goal is to train the neural network to make P'' as similar as possible to P' , which is formulated as

$$\theta^* = \operatorname{argmin}_{\theta} \frac{1}{N} \sum_{i=0}^{N-1} L(f_{\theta}(P_i), P'_i), \quad (1)$$

where θ refers the parameters of the neural network. $L(\cdot)$ is the loss function. N is the number of training samples. After training, we will obtain the optimal parameter θ^* .

IV. DATASET ACQUISITION

The acquisition of large-scale datasets is an essential prerequisite for deep learning-based error prediction algorithms. However, as far as we know, no public dataset has been established yet. To fill this gap, we introduce a data processing flow and manually collect a dental crown dataset in this paper.

Each sample in the dataset consists of a nominal dental crown model and its corresponding deformed model. The

nominal models are obtained in cooperation with hospitals and denture factories, which are designed by specialized skilled workers and saved as a stereolithography (STL) file. The deformed models are manufactured by a high-precision DLP 3D printer with fixed printing parameters and materials. Specifically, multiple nominal models are first imported into ten dimensional technology 3D printer software and laid out. Then, support structures are automatically added to the models using the software to prevent parts with overhanging structures from collapsing when printing. Afterward, the slicing operation is performed and the images are generated for fabrication. The photosensitive resin material is cured by a photopolymerization reaction under the action of the light source, forming a thin layer of the part. After the part is manufactured, post-processing operations, including manual cleaning and removal of support structures, are performed to obtain the fabricated dental crown models.

The following important step is to measure and store the manufactured dental crown models in a computer-recognizable format. For this purpose, we utilize the high-precision OKIO 3M-100 3D scanner, which contains a binocular camera and adopts a non-contact surface scanning method. The measurement accuracy can reach 0.007 mm. The data flow diagram for dataset acquisition is shown in Fig. 1. We place the deformed models to be scanned on a turntable with marking points, and the images taken by the binocular cameras are processed by specific software to obtain a partial point cloud of the target and the background. To obtain the complete point cloud, we turn the turntable to scan and measure from multiple views and then stitch the results. Considering that some of the structures are occluded, we flip the crown model manually and repeat the above process. As shown in Fig. 1, two results of unilateral scans consisting of the object and background are marked in orange and blue, respectively. Next, we separate the object from the background. It is observed that the object and background are not connected and the result of a unilateral scan consists of multiple high-density regions. A natural idea is to apply the density-based spatial clustering of applications with noise (DBSCAN) [15], which is a density clustering-based algorithm that divides regions with sufficient density into clusters. Finally, the cluster with the largest size is automatically chosen as the object.

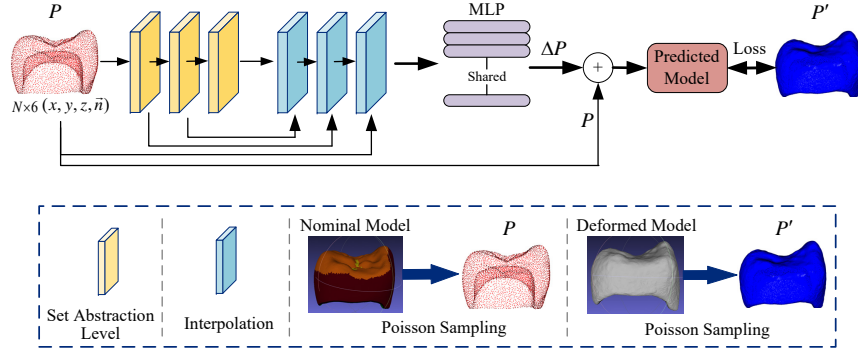


Fig. 2. The architecture of the proposed neural network

After obtaining the two partially scanned crown models, we apply the iterative closest point (ICP) algorithm [16] to combine them into a complete one. Since the overlap between the two scanned parts is small, we need to find a good initial transformation matrix. To this end, the nominal model and the partially scanned crown models are first moved to the coordinate origin. Then the RANSAC-based global registration [17] is performed between the nominal model and the scanned model to obtain the initial rough transformation matrix. To further improve the accuracy of point cloud registration, point-to-plane ICP is utilized to perform global registration. At this time, the two partially scanned crown models are brought into a roughly matched position. Further, the ICP-based global registration algorithm and the merging operation are performed on the two partially scanned models to obtain the complete deformed model. The merging operation mainly consists of the following steps: 1) Sampling on the surfaces of the two models, and then concatenating the sampled point clouds; 2) Estimating the normal vectors of the points and then performing surface reconstruction using the Poisson reconstruction algorithm. Finally, the best fit alignment algorithm is performed between the deformed model and the nominal model. In this way, the sum of squares of distances between the sample pairs from the two models is minimized.

V. ERROR PREDICTION METHOD

In this paper, we adopt a neural network based on PointNet++ [18], which is an improved version of PointNet [19]. It performs the hierarchical feature extraction that PointNet ignores. For a local region, PointNet is first applied to capture the local geometry of the point cloud and the interactions between points. Then similar to CNNs, the input data is subsampled several times for features aggregation from larger local regions until the features of the whole point set are captured. Fig. 2 shows the overall architecture of the proposed neural network. It can be observed that the input is a nominal point cloud $P \in \mathbb{R}^{N \times 6}$, where N is the number of points, and each point has a 3-dimensional x - y - z coordinate vector and a normal vector. The input is first fed to three set abstraction levels for feature extraction. After obtaining point-wise features for all original points, a shared

multilayer perceptron (MLP) is utilized to predict deviations for all points. Finally, the predicted deviations are added to the coordinates of the original points to obtain the predicted model. A loss between the predicted model and the deformed model is calculated and used for parameter learning.

A set abstraction level takes an $N \times (d + C)$ matrix as input, where N is the number of points, and each point is with d -dim coordinates and C -dim point features. It outputs an $N_o \times (d + C_o)$ matrix of N_o subsampled points with d -dim coordinates and new C_o -dim feature vectors that summarize the local context. A set abstraction level consists of a sampling layer, a grouping layer, and a PointNet layer. In the sampling layer, the farthest point sampling algorithm is iteratively used to obtain a subset of the input point set. For each sampled point x_c , the grouping layer finds its local region, which consists of points within a radius centered at x_c . After that, the PointNet layer encodes local region patterns into a feature vector \mathbf{f}_c , which can be calculated as

$$\mathbf{f}_c = \text{MAX}_{i=1, \dots, k} \{g([\{x_i - x_c\}, \mathbf{f}_{x_i}])\}, \quad (2)$$

where $\{x_1, x_2, \dots, x_k\}$ is a point set in the local region, k is the number of points, and $\{\mathbf{f}_{x_1}, \mathbf{f}_{x_2}, \dots, \mathbf{f}_{x_k}\}$ is a feature set of these points. $[\cdot]$ represents a concatenation operation. All the points are transformed to a local coordinate system with the centroid as the origin and then concatenated with their corresponding feature vectors. The results are fed into g for feature transformation. g is usually an MLP followed by a batch normalization (BN) layer and a rectified linear unit (ReLU) activation function with shared parameters across all regions and points. Finally, a max-pooling function is used as a symmetric function to aggregate features of all points in the local region into a latent vector. The vector stores the global contextual information about the input geometry.

In the error prediction task, we need to obtain the point-wise features for each point in the input and predict its deviation. However, the original point set is subsampled in the set abstraction level. Therefore, we propagate features from subsampled points to the original points by interpolation. Assume that the layer l is with the shape of $N_l \times (d + C_l)$, and the layer $l - 1$ is with the shape of $N_{l-1} \times (d + C_{l-1})$, where N_l and N_{l-1} are number of points. A distance-based interpolation method is adopted. Specifically, for each

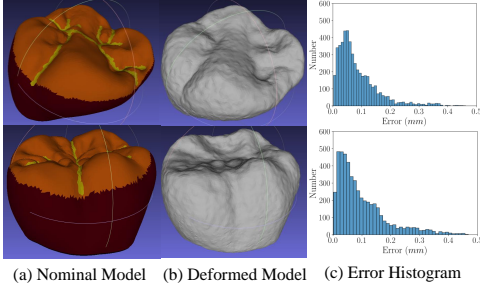


Fig. 3. Two samples of the dataset

point x among N_{l-1} points, we find its k nearest neighbors from the set of N_l points, and then use inverse distance weighted average based on the k nearest neighbors to obtain interpolated feature values $\mathbf{f}'(x)$, i.e.,

$$\mathbf{f}'(x) = \frac{\sum_{i=1}^k w_i(x) \mathbf{f}_{x_i}}{\sum_{i=1}^k w_i(x)}, \text{ and } w_i(x) = \frac{1}{E(x, x_i)^q}, \quad (3)$$

where x_i is the i th nearest neighbor among N_l points of x , and \mathbf{f}_{x_i} is the feature of x_i . w is the weight, which is determined by the Euclidean distance E between x and x_i and a hyper-parameter q . In the experiment, we use $q = 2$ and $k = 3$ by default. After obtaining $\mathbf{f}'(x)$, we concatenate it with the feature of x , and then apply an MLP to reduce the feature dimension.

In the experiment, the mean squared error (MSE) is adopted as the loss function, which can be calculated as

$$L = \frac{1}{N} \sum_{i=1}^N (p_i - p'_i)^2, \quad (4)$$

where p_i is a point in the nominal point cloud, and p'_i is its corresponding point in the deformed point cloud. N is the number of points in the nominal point cloud.

VI. EXPERIMENTS

A. Dataset

Following the data processing flow described in Section IV, we collect a total of 82 samples, each of which consists of a pair of nominal and deformed models. In this section, we describe how the acquired dataset is further processed to verify the performance of the neural network.

We perform Poisson sampling on the surface of the nominal model V and deformed model V' to obtain point clouds P and P' , respectively. For a point p in P , we regard its corresponding point as the one that has the closest Euclidean distance to it in P' . Therefore, we sample 8,000 points on the surface of the nominal model and 1,000,000 points on the surface of the deformed model. The distance between each pair of points is calculated to find the correspondence between the points. Finally, 5,000 corresponding points are randomly selected as the input and ground truth of the neural network. Fig. 3 shows two samples of the dataset. In Fig. 3 (c), the x -axis represents the size of the errors in millimeters, and the y -axis represents the number of points.

To eliminate the effect of an unbalanced data partition, we perform three-fold cross-validation. The samples in the dataset are divided into three mutually exclusive subsets of similar size. One of them is extracted each time as the test set, and the remainings are used as the training set. The average result on multiple test sets is used to evaluate the performance of the model.

Considering that the sample size is not large, data enhancements are performed on the training set to improve the performance of the proposed network. First, the coordinates of all samples are transformed to $(-1, 1)$ according to a fixed scale. Then the following operations are performed for all training samples: 1) Translation: Translate randomly by a distance of $(0, 0.1)$ along the x , y and z axes; 2) Rotation: Rotate by a random angle along the z axis; 3) Downsampling: Sample 5,000 points randomly in the nominal point cloud as the input of the neural network; 4) Flipping: Flip the point cloud randomly along the x and y axes.

B. Metric

At the training stage, for a point in the nominal point cloud P , the point with the closest distance to it in the deformed point cloud P' is regarded as its corresponding point. When testing, the original correspondence is no longer used. Alternatively, we recalculate the corresponding point from the deformed point cloud for each item of the predicted point cloud, and adopt the average value of Euclidean distance as the metric. Therefore, the metric function is

$$D = \frac{1}{|P''|} \sum_{u \in P''} \min_{v \in P'} \|u - v\|_2, \quad (5)$$

where P'' is the predicted point cloud, and P' is the deformed point cloud. For a point u in P'' , it finds the nearest point v in P' , and then calculates the average Euclidean distance.

C. Results and Analysis

The experiment is conducted on a workstation with an Intel Xeon E5-2698 v4 CPU and a Titan V100 Graphics Processing Unit. The neural network is implemented by using the PyTorch framework and trained by the Adam optimizer. In Table I, the quantified errors of the nominal-deformed and predicted-deformed model pairs are shown. The size of the dental crown is about 13 mm, and the average errors between nominal-deformed and predicted-deformed model pairs are 0.0763 mm and 0.0368 mm, respectively. It proves that the proposed method can achieve promising error prediction results. Also, the results of the three-fold cross-validation are similar, which indicates that there is almost no effect caused by the unbalanced data set partition. To show the results more intuitively, the visualization results are given in Fig. 4, where (a) and (c) show the errors between nominal and deformed models, (b) and (d) show the errors between predicted and deformed models. Different colors are utilized to distinguish the magnitude of the errors, and the correspondence between the error values and the colors is shown in the colormap. It can be observed that the neural

TABLE I
ERROR PREDICTION RESULTS IN AM (MILLIMETER)

Error	Errors between nominal and deformed models	Errors between predicted and deformed models
The first fold	0.0761	0.0368
The second fold	0.0771	0.0371
The third fold	0.0758	0.0366
Average	0.0763	0.0368

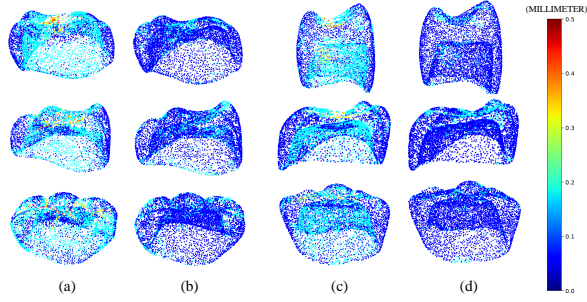


Fig. 4. Visualization results for error prediction, where (a) and (c) show the errors between nominal and deformed models, and (b) and (d) show the errors between predicted and deformed models.

network is able to predict most of the errors. However, the prediction accuracy is lower at the upper surface and bottom edge of the crown model. Part of the reason is that the removal of supports damages the surface structure on the upper surface. Also, the curvature of the bottom edge of the dental crown model is large and fewer points are scanned, resulting in partial distortion during reconstruction. Therefore, it is essential to further improve the quality of the collected dataset.

Computational efficiency is an important aspect in assessing the performance of a method. Our model has 1.4 million trainable parameters. As for the time efficiency, it takes 7.6 milliseconds on average to predict the deformation of a 3D model. About 132 predictions can be done in one second. The above results demonstrate the high computational efficiency of our method.

VII. CONCLUSIONS

In this paper, we propose a point-based network for error prediction in AM. The proposed method extracts multi-level and multi-scale contextual features for each point to predict the deviation, which can greatly alleviate the memory burden caused by the voxel-based approaches. We conduct experiments on a real-scenario dataset and the results show that the proposed method achieves promising performance. In this work, the quality of the dataset is critical. Besides support structure removal and inaccurate scanning, errors from the registration of two unilateral scans can affect the accuracy of the deformed model. As future work, collecting a larger size and higher quality dataset is desirable. Also, it is worthwhile to explore self-supervised learning to enhance the understanding of 3D models by neural networks, and thus

improve the performance of few-shot learning. Moreover, only error prediction is performed in this paper, and error compensation will be tested in the system.

REFERENCES

- [1] S. Chowdhury and S. Anand, "Artificial neural network based geometric compensation for thermal deformation in additive manufacturing processes," in *International Manufacturing Science and Engineering Conference*, vol. 49910, 2016, p. V003T08A006.
- [2] R. Hong, L. Zhang, J. Lifton, S. Daynes, J. Wei, S. Feih, and W. F. Lu, "Artificial neural network-based geometry compensation to improve the printing accuracy of selective laser melting fabricated sub-millimetre overhang trusses," *Additive Manufacturing*, vol. 37, p. 101594, 2021.
- [3] Z. Shen, X. Shang, M. Zhao, X. Dong, G. Xiong, and F.-Y. Wang, "A learning-based framework for error compensation in 3D printing," *IEEE Transactions on Cybernetics*, vol. 49, no. 11, 2019.
- [4] M. Zhao, G. Xiong, X. Shang, C. Liu, Z. Shen, and H. Wu, "Nonlinear deformation prediction and compensation for 3D printing based on CAE neural networks," in *2019 IEEE 15th International Conference on Automation Science and Engineering (CASE)*, 2019, pp. 667–672.
- [5] S. Westbeek, J. J. Remmers, J. van Dommelen, H. H. Maalderink, and M. G. Geers, "Prediction of the deformed geometry of vat photopolymerized components using a multi-physical modeling framework," *Additive Manufacturing*, vol. 40, p. 101922, 2021.
- [6] Q. Zhang, S. Weng, C. M. Hamel, S. M. Montgomery, J. Wu, X. Kuang, K. Zhou, and H. J. Qi, "Design for the reduction of volume shrinkage-induced distortion in digital light processing 3D printing," *Extreme Mechanics Letters*, vol. 48, p. 101403, 2021.
- [7] Q. Huang, J. Zhang, A. Sabbaghi, and T. Dasgupta, "Optimal offline compensation of shape shrinkage for three-dimensional printing processes," *IIE Transactions*, vol. 47, no. 5, pp. 431–441, 2015.
- [8] Q. Huang, H. Nouri, K. Xu, Y. Chen, S. Sosina, and T. Dasgupta, "Statistical predictive modeling and compensation of geometric deviations of three-dimensional printed products," *Journal of Manufacturing Science and Engineering*, vol. 136, no. 6, 10 2014.
- [9] H. Luan and Q. Huang, "Prescriptive modeling and compensation of in-plane shape deformation for 3-D printed freeform products," *IEEE Transactions on Automation Science and Engineering*, vol. 14, no. 1, pp. 73–82, 2016.
- [10] Y. Jin, S. J. Qin, and Q. Huang, "Modeling inter-layer interactions for out-of-plane shape deviation reduction in additive manufacturing," *IIE Transactions*, vol. 52, no. 7, pp. 721–731, 2020.
- [11] A. Sabbaghi, Q. Huang, and T. Dasgupta, "Bayesian model building from small samples of disparate data for capturing in-plane deviation in additive manufacturing," *Technometrics*, vol. 60, no. 4, pp. 532–544, 2018.
- [12] Q. Huang, Y. Wang, M. Lyu, and W. Lin, "Shape deviation generator—A convolution framework for learning and predicting 3-D printing shape accuracy," *IEEE Transactions on Automation Science and Engineering*, vol. 17, no. 3, pp. 1486–1500, 2020.
- [13] Y. Wang, C. Ruiz, and Q. Huang, "Extended fabrication-aware convolution learning framework for predicting 3D shape deformation in additive manufacturing," in *2021 IEEE 17th International Conference on Automation Science and Engineering*, 2021, pp. 712–717.
- [14] J. Francis and L. Bian, "Deep learning for distortion prediction in laser-based additive manufacturing using big data," *Manufacturing Letters*, vol. 20, pp. 10–14, 2019.
- [15] M. Ester, H.-P. Kriegel, J. Sander, and X. Xu, "Density-based spatial clustering of applications with noise," in *Int. Conf. Knowledge Discovery and Data Mining*, vol. 240, no. 6, 1996.
- [16] Y. Chen and G. Medioni, "Object modelling by registration of multiple range images," *Image and vision computing*, vol. 10, no. 3, pp. 145–155, 1992.
- [17] Q.-Y. Zhou, J. Park, and V. Koltun, "Fast global registration," in *European Conference on Computer Vision*, 2016, pp. 766–782.
- [18] C. R. Qi, L. Yi, H. Su, and L. J. Guibas, "PointNet++: Deep hierarchical feature learning on point sets in a metric space," in *Advances in Neural Information Processing Systems*, 2017, pp. 5099–5108.
- [19] C. R. Qi, H. Su, K. Mo, and L. J. Guibas, "PointNet: Deep learning on point sets for 3D classification and segmentation," in *IEEE Conference on Computer Vision and Pattern Recognition*, 2017, pp. 652–660.